Magill, C. R., Eglinton, G., & Eglinton, T. I. (2019). Isotopic variance among plant lipid homologues correlates with biodiversity patterns of their source communities. *PLoS ONE*, *14*(2), [e0212211]. https://doi.org/10.1371/journal.pone.0212211

PLOS ONE

RESEARCH ARTICLE

# Isotopic variance among plant lipid homologues correlates with biodiversity patterns of their source communities

**Clayton R. Magill**[1,2]*, **Geoffrey Eglinton**[3†], **Timothy I. Eglinton**[2]

**1** Lyell Centre, Heriot-Watt University, Edinburgh, United Kingdom, **2** Geological Institute, ETH Zürich, Zurich, Switzerland, **3** Department of Earth Sciences, University of Bristol, Bristol, United Kingdom

† Deceased.
* C.Magill@hw.ac.uk





**Citation:** Magill CR, Eglinton G, Eglinton TI (2019) Isotopic variance among plant lipid homologues correlates with biodiversity patterns of their source communities. PLoS ONE 14(2): e0212211. https://doi.org/10.1371/journal.pone.0212211

**Editor:** Paul C. Struik, Wageningen University, NETHERLANDS

**Received:** August 31, 2018

**Accepted:** January 29, 2019

**Published:** February 27, 2019



**Data Availability Statement:** All relevant data are within the manuscript and its Supporting Information files.

**Funding:** This work was funded through H2020 Marie Skłodowska-Curie Actions (FEL-30 12-2; http://ec.europa.eu/programmes/horizon2020/en/h2020-section/marie-sklodowskacurie-actions) awarded to C.R.M., but funders played no role in the conception or completion of this work.

**Competing interests:** The authors have declared that no competing interests exist.

## Abstract

Plant diversity is important to human welfare worldwide, and this importance is exemplified in subtropical and tropical [(sub)tropical] African savannahs where regional biodiversity enhances the sustaining provision of basic ecosystem services available to millions of residents. Yet, there is a critical lack of knowledge about how savannahs respond to climate change. Here, we report the relationships between savannah vegetation structure, species richness, and bioclimatic variables as recorded by plant biochemical fossils, called biomarkers. Our analyses reveal that the stable carbon isotope composition ($\delta^{13}C$) of discrete sedimentary plant biomarkers reflects vegetation structure, but the isotopic range among plant biomarkers–which we call LEaf Wax Isotopic Spread (LEWIS)–reflects species richness. Analyses of individual biomarker $\delta^{13}C$ values and LEWIS for downcore sediments recovered from southeast Africa reveal that the region's species richness mirrored trends in atmospheric carbon dioxide concentration ($pCO_2$) throughout the last 25,000 years. This suggests that increasing $pCO_2$ levels during post-industrialization may prompt future declines in regional biodiversity (1–10 species per unit $CO_2$ p.p.m.v.) through imminent habitat loss or extinction.

## Introduction

Observations and basic ecological theory provide corroborative support that diverse ecosystem services in savannahs are maintained by plant diversity [1, 2]. Yet, decades of research still leave some outstanding questions about African savannah dynamics during past intervals of dramatic climate changes (e.g., deglaciation) [3–5], and the consequences of human activities on regional biodiversity are a source of debate [6]. This debate continues, in part, because of lacking (paleo)biodiversity proxies applicable across multiple scales and key geologic archives [7]. For instance, although many (paleo)vegetation reconstructions employ pollen spectra as a metric of biodiversity [8], uncertainties surrounding pollen dispersal dynamics [9] and taphonomy [10] impose significant limitations on its use as a robust biodiversity proxy [7]. Additionally, pollen is largely reflective of fecundity as opposed to species abundance,

distribution, and biomass [11]. As such, developing practical biodiversity proxies represents an urgent task for scientists and legislators alike as anthropogenic climate change intensifies [12].

Savannah vegetation communities are characterized by quick, nonlinear succession dynamics and threshold transitions [13] among grasses, woody plants and forbs [14–16]. The dominance of these coexisting plant functional types (PFTs) is reflected by physiognomic classifications of African savannah ecosystem structure as related to woody plant (crown) cover (c.f., Discussion A in S1 File), which defines understory gradients in resources [17], such as water, nutrients, and light [18, 19]. Ecosystem structure in turn influences underlying plant biodiversity patterns in savannahs [19, 20], but the nature of this influence is subject to differences in source accumulation area and time (i.e., scale) [21] and biogeographic variables, such as ecoregion extent [22, 23].

Conceptually, plant biodiversity is a measure of both species abundance (richness) and distribution (evenness) at the regional, landscape, and local level [21]. However, plant species richness (PSR) functions as a common index of biodiversity [1, 22] because of its strong positive relationships with resource-use differentiation [24] and functional trait divergence (e.g., growth habit) [14] among plants.

PFTs closely parallel functional trait divergence [25], which defines alternative strategies for mitigating pervasive resource constraints on and during plant development [26]. Associated functional traits include any phenotypic or chemical feature impacting plant fitness and their interactions with the environment [27], and thus describe vegetation dynamics with respect to ecophysiological factors [28] as opposed to strict taxonomic associations [14]. For instance, in southeast African savannah vegetation communities, a combination of divergent life strategies and taxonomic (i.e., species) richness account for most foliar chemical diversity [17], which in turn strongly parallels contemporary plant biodiversity [29]. As such, PFT-based techniques are reliably powerful for reconstructing plant biodiversity patterns alongside or in lieu of traditional taxonomic approaches (e.g., pollen spectra) [30].

Refractory plant biomarkers, such as most long-chain *n*-alkanes, in soils and terrestrial deposits exhibit molecular and isotopic signatures that reflect bioclimatic conditions during plant development [31]. Biomarker *n*-alkanes, in particular, are major molecular constituents of the waxy protective cuticle covering plant leaves [32, 33] that have characteristic odd-numbered $C_{27}$–$C_{33}$ homologue distributions in different PFTs [34]. High abundances of $C_{33}$ *n*-alkanes (*n*-$C_{33}$) characterize many grasses and forbs in modern savannahs [32], and higher *n*-$C_{27}$ and *n*-$C_{29}$ abundances characterize woody plants [33]. The stable carbon isotopic composition of biomarker *n*-alkanes, expressed here as $\delta^{13}C$ values, are also characteristic in different PFTs, wherein $C_4$ grasses have much higher values than woody plants and forbs with $C_3$ photosynthesis [ca. –20‰ and –35 ±5‰, respectively (S1 Table)]. Among plants with $C_3$ photosynthesis, biomarker *n*-alkane $\delta^{13}C$ values decrease with higher resource availabilities and shade [35]. As such, biomarker *n*-alkane $\delta^{13}C$ values serve as a uniquely quantitative reflection of PFT dominance [35], and thus ecosystem structure [16, 17], in savannahs across space and through time [36].

We report here on a new approach for estimating (paleo)biodiversity in savannahs, developed from new and literature data on biomarker *n*-alkane signatures in contemporary plants, surface soils and terrestrial deposits derived from (sub)tropical African sources. This approach builds on earlier studies relating plant biodiversity with (i) tree cover [20], (ii) PFT dominance [15], and (iii) biomarker *n*-alkane signatures [35–38] to develop predictive relationships connecting plant species richness and biomarker *n*-alkane signatures in savannahs. Then, we extend these contemporary predictive relationships to marine sediment biomarker *n*-alkane records off the Zambezi River mouth (Fig 1) [39, 40] to reconstruct biodiversity patterns in southeast Africa since ~25 thousand years ago (kya).

## Materials and methods

### Contemporary plants

We compiled both new and literature data of $C_{27}$–$C_{33}$ *n*-alkane $\delta^{13}C$ values in contemporary plant leaves [$n$ = 139 (Fig 2; S1 Table)] from at least 82 distinct species representative of the

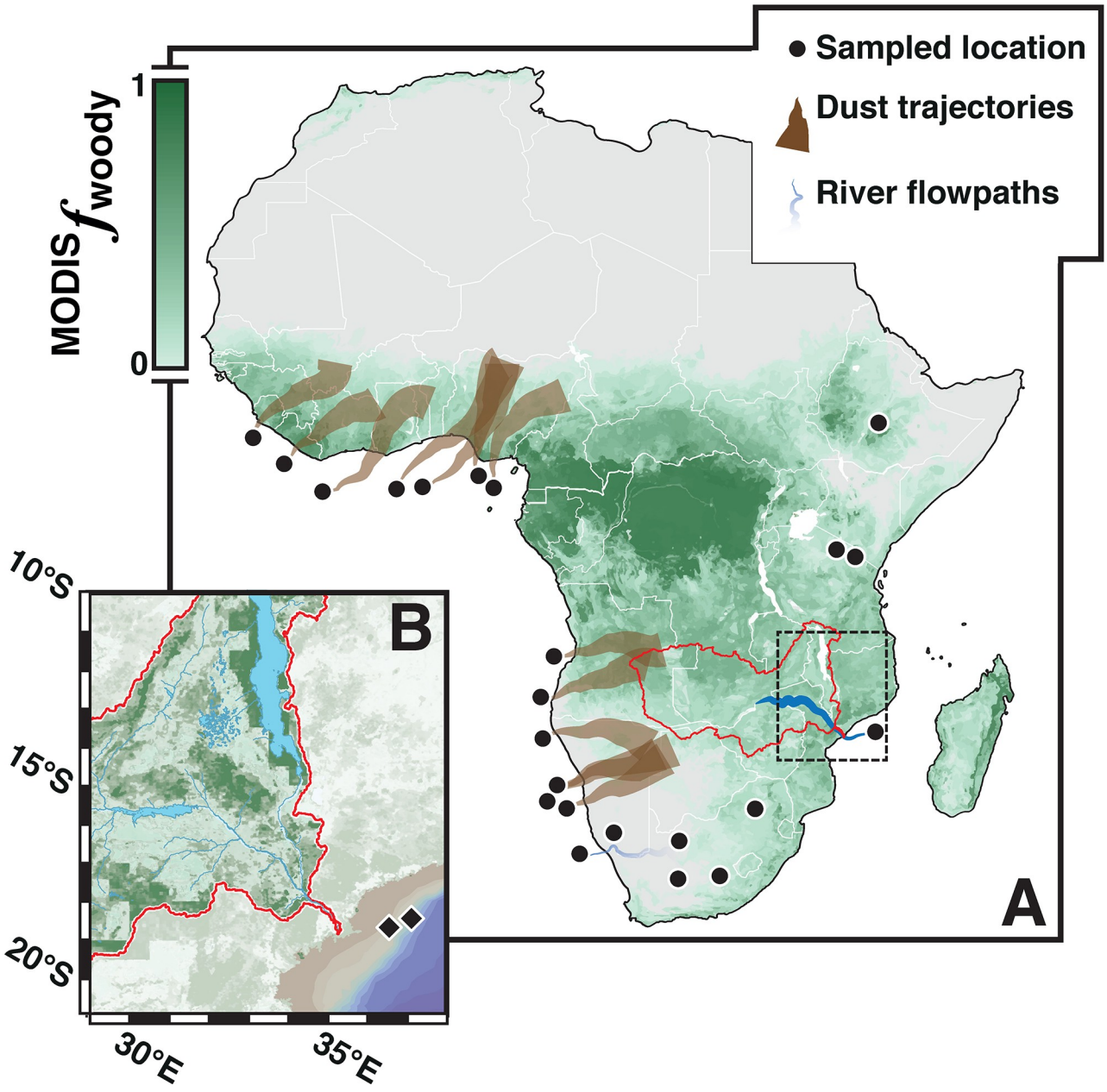


**Fig 1. Satellite-estimated fractional tree cover and locations of the samples used for surface-sediment biomarker analyses (black circles). A**, Satellite estimates of fractional tree cover ($^{MODIS}f_{woody}$) throughout (sub)tropical Africa [66]. Satellite data (available at landcover.org/data/) was resampled from 30-m resolution at 0.05˚ in ArcGIS 10.2.1 for improved figure visualization. Lighter-to-dark shading (green) represents increased fractional tree cover. Surface-sediment back-trajectories were constrained by geomorphological features, river discharge data, and Lagrangian atmospheric circulation models (Discussion D in S1 File). The Zambezi River catchment is outlined in red. **B**, Zoom-in of fractional tree cover estimates in the lower Zambezi sub-catchment (c.f., black dashed box in Fig 1A for map position). Black diamonds mark the marine sites used for sediment biomarker analyses: GeoB9307-3 [18˚34.0'S, 37˚22.9'E (542 m water depth)] [39], GIK16160 [18˚14.5'S, 37˚52.1'E (1339 m water depth)] [40].

https://doi.org/10.1371/journal.pone.0212211.g001

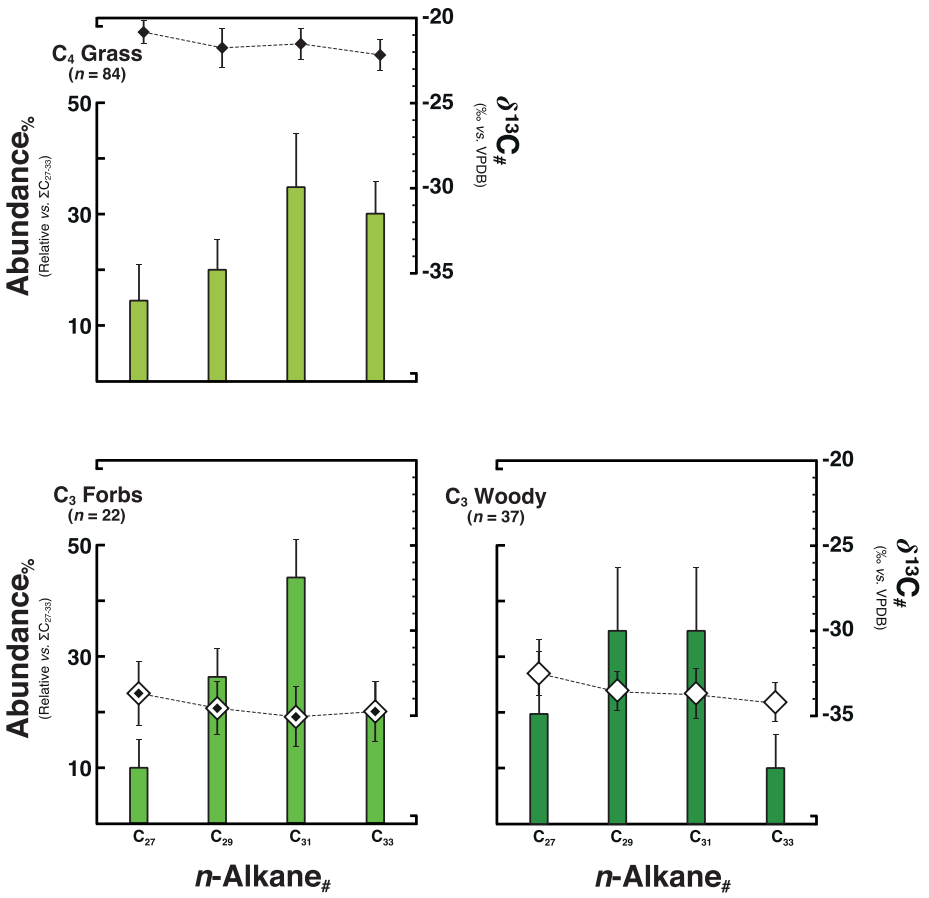


**Fig 2. Compiled leaf-wax *n*-alkanes signatures of contemporary plants.** Compiled leaf-wax *n*-alkanes signatures of 139 contemporary plants, which represent 82 distinctive species of (sub)tropical African savannah vegetation communities (S1 Table). Plants were separated by photosynthetic pathway and growth habit into one of three overarching plant functional types (PFTs): $C_3$ woody ($n = 42$), $C_3$ forbs ($n = 22$), and $C_4$ grass ($n = 75$). Stable carbon isotopic values of $C_{27}$–$C_{33}$ *n*-alkanes ($\delta^{13}C_{\#}$) are shown as medians with their median absolute deviation (±MAD). Histograms depict the relative abundance of $C_{27}$–$C_{33}$ *n*-alkanes in each PFT (median±MAD).

https://doi.org/10.1371/journal.pone.0212211.g002

commonest African savannah vegetation communities (Discussion B in S1 File) [14–16]. To account for within and between-species isotopic variations caused by plasticity [41], appertaining plants were assigned to one of three dominant PFTs based on photosynthetic pathway and growth habit [15]: $C_3$ woody plants ($n = 42$), $C_3$ forbs ($n = 22$), and $C_4$ grasses [$n = 75$ (Discussion B in S1 File)].

For new data, we collected fresh leaves and B-horizon soils during boreal summer of 2011 to complement the molecular and isotopic data reported by previous studies (S1 and S2 Tables). Fresh leaves [$n = 44$ (S1 Table)] were sampled from at Ngorongoro Conservation Area and the surrounding park (3.5±0.5˚S, 35.0±1.0˚E) together with correlative soil B-horizons [$n = 11$ (S2 Table)], which were sampled following protocols of Belsky *et al.* [17] from depths of 0–2.5 cm underneath surface soil (O/A horizon) layers. Corresponding permits were issued for regions around Olduvai Gorge (Arusha) by the Tanzania Wildlife Research Institute (TAWIRI) through the Commission for Science and Technology (COSTECH). Freeze-dried leaves or soils were mechanically powdered before accelerated solvent extraction (ASE) with dichloromethane:methanol [DCM:MeOH (85:15 v/v)] in a sequence of three cycles of 5 min at 10.3 MPa and 100˚C with 70% flush volume [42]. Resultant total lipid extracts were evaporated

to dryness under nitrogen, reconstituted in 50 μl of the extraction solvent, and then allowed to evaporate in a second ASE packed with 1 g quartz sand, 2 g of 5% (w/w) silver-impregnated silica gel, and 6 g activated silica gel [42]. Once evaporated, the unsaturated hydrocarbons (e.g., *n*-alkanes) were separated from associated total lipid extracts via selective, sequential ASE with hexane in one cycle of 1 min at 3.4 MPa and 50˚C with 30% flush volume [42].

Once separated, the unsaturated hydrocarbons were characterized first by gas chromatography (GC) flame ionization detection on a HP 5890 [60-m HP5 (0.32 mm × 0.25 μm)]; GC temperature was set to 60˚C for 1 min, ramped to 320˚C at 6˚C $min^{-1}$, and held for an additional 20 min at 320˚C. Thereafter, unsaturated hydrocarbons were measured by gas chromatography (combustion) isotope-ratio monitoring mass spectrometry on a Thermo TraceGC Ultra [60-m HP5 (0.32 mm × 0.25 μm)] and Thermo DeltaV Plus connected via a continuous flow interface using the same oven-ramp program as with GC-FID. Samples were injected in splitless mode and turned to carbon dioxide via combustion over nickel and platinum wire in helium at 1000˚C. Stable carbon isotopic values are expressed in standard permil (‰) notation relative to Vienna Pee Dee Belemnite (VPDB):

$$\delta^{13}C = 1000\left(\frac{R_{sample}}{R_{standard}} - 1\right);\ R = \frac{^{13}C}{^{12}C}$$

Within-run precision (1σ) and accuracy were determined from co-injected lipids of known concentration and isotopic composition (c.f., Schimmelmann Standard B4) and have values of 0.11‰ and 0.10‰ ($n = 88$), respectively.

### Soils and terrestrial deposits

We also compiled biomarker *n*-alkane $\delta^{13}C$ values ($n = 40$) for (sub)tropical African samples of terrestrial-derived fine-grain materials often incorporated into sedimentary geologic archives [i.e., sediments, soil, litter and dust; hereafter, "surface sediments" (S2 Table)]. These surface sediments were selected to reflect the major source-to-sink transport histories of biomarker *n*-alkanes (Discussions C and D in S1 File) [43] for (sub)tropical Africa and its spectrum of diverse savannah ecosystems, spanning grassland to woodland [16].

## Results

### Contemporary plants

Altogether, contemporary plants show significant differences in associated $C_{27}$–$C_{33}$ *n*-alkane $\delta^{13}C$ ($\delta^{13}C_{27-33}$) values within and between dominant PFTs (Fig 2). In contrast, the average range of $\delta^{13}C_{27-33}$ values in individual leaves is about 1.9‰ for all the dominant PFTs (S1 Table). To represent this isotopic range across a homologous series of compounds, we introduce an index called LEaf-Wax Isotopic Spread (LEWIS):

$$\text{LEWIS} = max|\delta^{13}C_{x-y}| - min|\delta^{13}C_{x-y}|$$

Here, $\delta^{13}C_{x-y}$ is representative of the $\delta^{13}C$ values in a regular series of homologous compounds with *x* through *y* carbons (e.g., $\delta^{13}C_{27-33}$ represents *n*-$C_{27}$, *n*-$C_{29}$, *n*-$C_{31}$, and *n*-$C_{33}$). In essence, associated LEWIS values represent the distribution-weighted PFT differences in carbon isotope discrimination among principle sources of biomarker *n*-alkanes in a sample [44], which is ideal for addressing plant functional trait divergence and biodiversity questions in complex ecosystems [45]. Although our study focuses on *n*-alkanes, in concept, LEWIS likewise could be applied to related homologous *n*-alkyl biomarkers, such as alcohols and fatty acids [37].

## Soils and terrestrial deposits

Surface-sediment $\delta^{13}C_{27-33}$ values show an inverse relationship with satellite and biomarker-estimated fractional tree cover of their source-vegetation communities (Fig 3). At first, $\delta^{13}C_{27-33}$ values were compared to estimates of MODerate-resolution Imaging Spectradiometer (MODIS) derived fractional tree cover of their inceptive source-vegetation communities in (sub)tropical Africa [$^{MODIS}f_{woody}$ (Fig 1 and Discussion D in S1 File)]. Although estimates of fractional tree cover show a significant linear relationship with the $\delta^{13}C$ values of $C_{27}$–$C_{33}$ biomarker *n*-alkanes as individual homologues (S2 Table), the relationship is strongest with $\delta^{13}C$ values of *n*-$C_{31}$ [$\delta^{13}C_{31}$ ($r = -0.939$; $p < 0.0001$)]. Yet, the regression residuals of this relationship create a distinctive unimodal distribution, which tracks the characteristically quadratic rise of $C_3$ forb biomass [19, 35] at intermediate levels of tree cover in savannahs [46]. To account for the effects of forbs on surface-sediment biomarker *n*-alkane signatures, we used $\delta^{13}C_{31}$ values to derive more representative estimates (i.e., reconstructions) of fractional tree cover [$^{31}f_{woody}$ (Fig 3A and Discussion E in S1 File)]. Biomarker reconstructions of fractional tree cover show a much stronger correlation with satellite-estimated fractional tree cover as compared to individual $\delta^{13}C_{27-33}$ values (Fig 3B):

$$^{31}f_{woody} = 0.940\ ^{MODIS}f_{woody} + 0.014 (r^2 = 0.927)$$

Combined, these regression analyses indicate surface-sediment $\delta^{13}C_{31}$ values reflect fractional tree cover in savannahs at timescales of biomarker *n*-alkane accumulation and turnover [47].

Surface-sediment LEWIS values show a wide range [~1.5–4.5‰ (Fig 3C and 3D)] that belies the consistent $\delta^{13}C_{27-33}$ values of individual leaves (Fig 2). Associated LEWIS values show a distinctive unimodal relationship with $\delta^{13}C_{31}$ values (Fig 3C) and $^{MODIS}f_{woody}$ estimates (Fig 3D) that further indicates surface-sediment LEWIS does not simply parallel trends in reciprocal $C_3/C_4$ dominance or savannah fractional tree cover, respectively (Discussions E–G in S1 File). Considered together, such nonlinear relationships indicate surface-sediment LEWIS tracks an ecological threshold in savannah vegetation communities [13] related to ecosystem structure via canopy–gap gradients in carbon [35], water [48], and light [17, 19], which together can drive substantial differences in absolute $\delta^{13}C_{27-33}$ values of individual leaves even within monospecific communities [49].

The unimodal relationship present between surface-sediment LEWIS values and fractional tree cover resembles closely patterns in resource variance (e.g., patch-scale spatial heterogeneities in carbon, water and light) along grassland-forest transitions [50]. In savannahs, resource variance increases with increased tree cover until it reaches a critical threshold [13]. Thereafter, resource variance decreases with further crown closure [19] alongside successive reductions in canopy–gap spatial heterogeneity [17, 50]. Although ecological thresholds are dynamic [16], resource variance in savannahs usually peaks at fractional tree cover of 0.25–0.45 [19, 24]. Given resource variance shows close correspondence with biodiversity patterns [16], it comes as no surprise that plant species richness in savannahs also usually peaks at fractional tree cover of ~0.35±0.10 (Figure A in S1 File) [19, 51].

Surface-sediment LEWIS values show a significant linear correlation ($r = 0.849$; $p < 0.0001$) with literature estimates of PSR ($S_{source}$) [22] for ecoregions of their main source-vegetation communities (Fig 4A and Discussion D in S1 File). Yet, the interpretive significance of this straight-line relationship is not immediately clear, as surface-sediments differ in "integration scale", defined by generalizable average areas [i.e., accumulation extent ($km^2$)] and times [i.e., sedimentation interval (kya)] for specific surface-sediment types [43, 52]. Therefore, we rescaled $S_{source}$ estimates using predictive models of the species-time-area relationship (STAR)

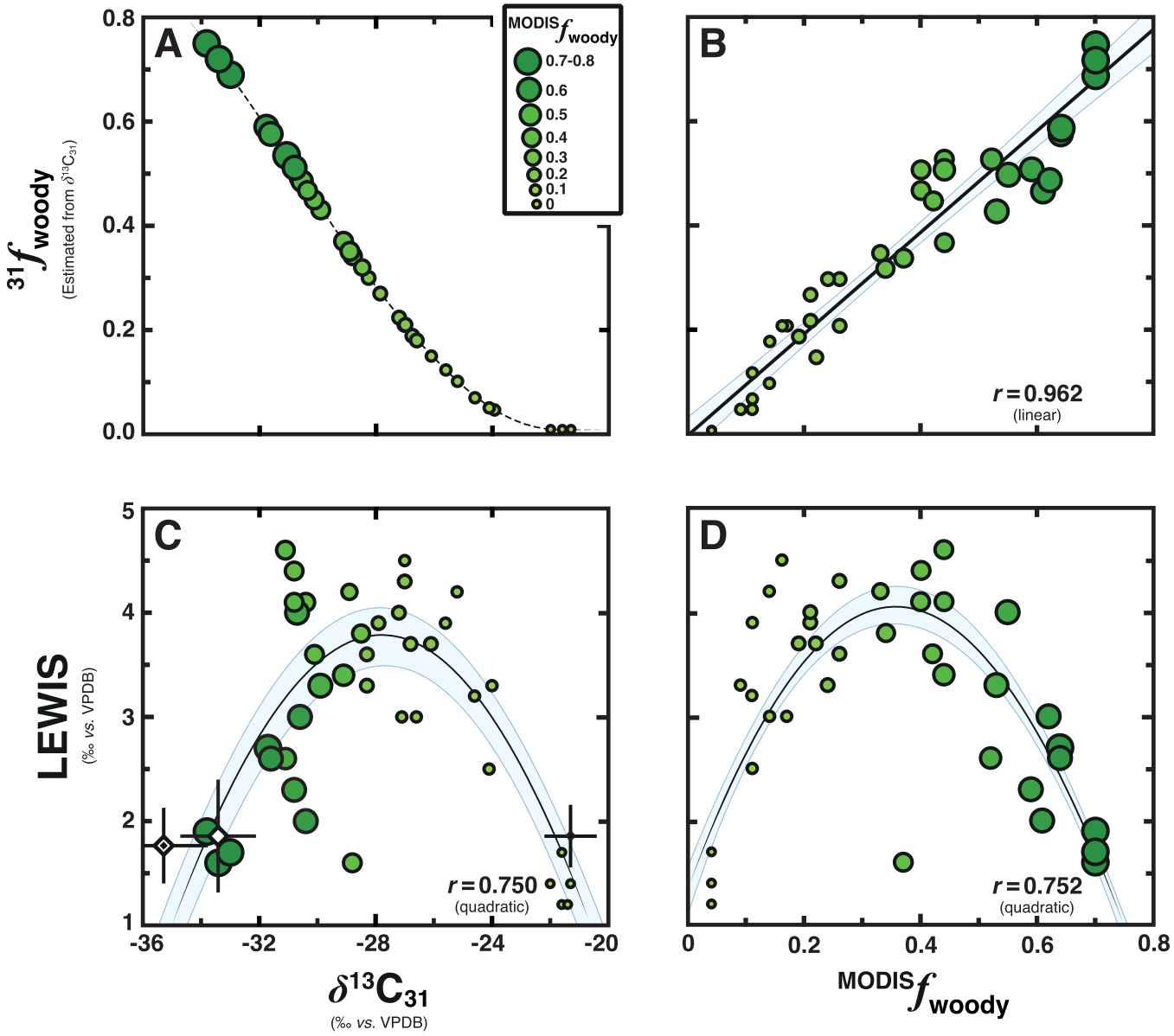


**Fig 3. Bivariate relationships shared between surface-sediment LEWIS, $\delta^{13}C_{31}$ values and fractional tree cover ($^{MODIS}f_{woody}$) estimates of (sub)tropical African source-region vegetation communities.** Larger circle sizes and darker shading (green) both represent increased fractional tree cover (c.f., Fig 1). Light blue shaded bounds indicate empirical 90% confidence intervals as calculated from a Monte Carlo method [92]. Asymptotic significance (*p*-value) is less than 0.0001 for all the relationships shown. **A**, Biomarker reconstructions of fractional tree cover ($^{31}f_{woody}$) were calculated from $\delta^{13}C_{31}$ values with a nonlinear equation [35]:

$$^{31}f_{woody} = \{sin(-1.8353 - 0.08538 \times \delta^{13}C_{31})\}^2$$

**B**, Biplot between satellite-estimated fractional tree cover ($^{MODIS}f_{woody}$) and biomarker-reconstructed fractional tree cover ($^{31}f_{woody}$). **C**, Relationship shared between surface-sediment LEWIS and $\delta^{13}C_{31}$ values. Also shown are median values and the median absolute deviation of dominant PFTs (S1 Table) [15]: $C_3$ woody plants [$n$ = 37 (white diamond)], $C_3$ forbs [$n$ = 22 (double diamond)], and $C_4$ grasses [$n$ = 84 (black diamond)]. **D**, Relationship shared between surface-sediment LEWIS values and fractional tree cover ($^{MODIS}f_{woody}$) estimates.

https://doi.org/10.1371/journal.pone.0212211.g003

[23] for modern savannahs (Discussion F in S1 File), which functions as a standardization method for species richness in samples (i.e., sediment types) with incommensurate integration scales [53].

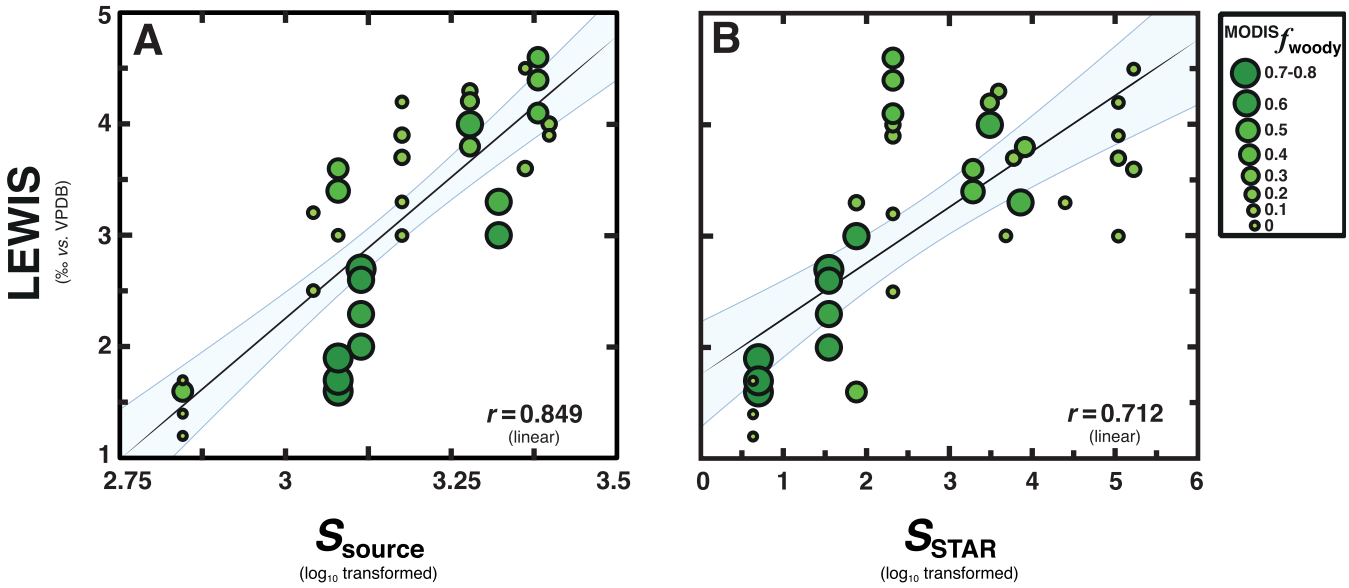


**Fig 4. Bivariate relationships shared between surface-sediment LEWIS values and the corresponding plant species richness (PSR) of their source-region vegetation communities.** Larger circle sizes and darker shading (green) both represent increased fractional tree cover ($^{MODIS}f_{woody}$) estimates (c.f., Fig 1). Solid lines represent linear regression models. Blue shaded bounds indicate empirical 90% confidence intervals as calculated from a Monte Carlo method [92]. Asymptotic significance (*p*-value) is less than 0.0001 for all the relationships shown. **A**, Biplot between surface-sediment LEWIS values and the ecoregion estimates of PSR ($S_{source}$) [22] for their main source-region vegetation communities (Discussion F in S1 File). **B**, Biplot between surface-sediment LEWIS values and (re)scaled PSR estimates using predictive models of the species-time-area relationship (STAR) [23] for modern savannahs [$S_{STAR}$ (Discussion F in S1 File)]. Note, we used log-transformed PSR for our analyses to improve data normality, minimize heteroscedasticity, and foster consistent linear relationships across disparate scales and datasets [1, 21, 23].

https://doi.org/10.1371/journal.pone.0212211.g004

Rescaled $S_{source}$ estimates–called *S*STAR–have a weaker correlation with surface-sediment LEWIS values as compared to simple ecoregion estimates of PSR (Fig 4B). Yet, the strength of this relationship grows much stronger after using partial bivariate regression models [54] to account for common covariance with fractional tree cover estimates [i.e., $^{MODIS}f_{woody}$ (Figure C in S1 File)], which in turn co-varies with bioclimatic variables such as rain and fire regime [18]. The consistent linear correlations shared between surface-sediment LEWIS values and PSR, despite differences in respective integration scales [43] and transmission dynamics [52], support the premise that LEWIS functions as a semi-quantitative index of biodiversity patterns.

## Discussion

With a calibration surface-sediment LEWIS framework established, we sought to reconstruct Afrotropical biodiversity patterns during previous intervals of far-reaching global warming, such as the last deglaciation [~21–7 kya]. Therefore, we examined previously reported $\delta^{13}C_{27-33}$ values in correlative marine cores recovered from off the mouth of the Zambezi River (Fig 1B) [39, 40], which is southern Africa's second largest river system. Once combined, these records offer complementary perspectives on the developing plant biodiversity of the lower Zambezi sub-catchment (Discussions G–I in S1 File) throughout the last ~25 kya that transcends any particular record taken alone (Fig 5A and 5C).

Biomarker records from marine [39, 40] and lake sediments [55] suggest there was a gradual long-term expansion of trees and bushes in southeast Africa during the LGM–Holocene transition. In contrast, pollen records and beta diversity patterns suggest that the community phylogenetic structure of Zambezian ecoregions remained the same or similar since at least 25

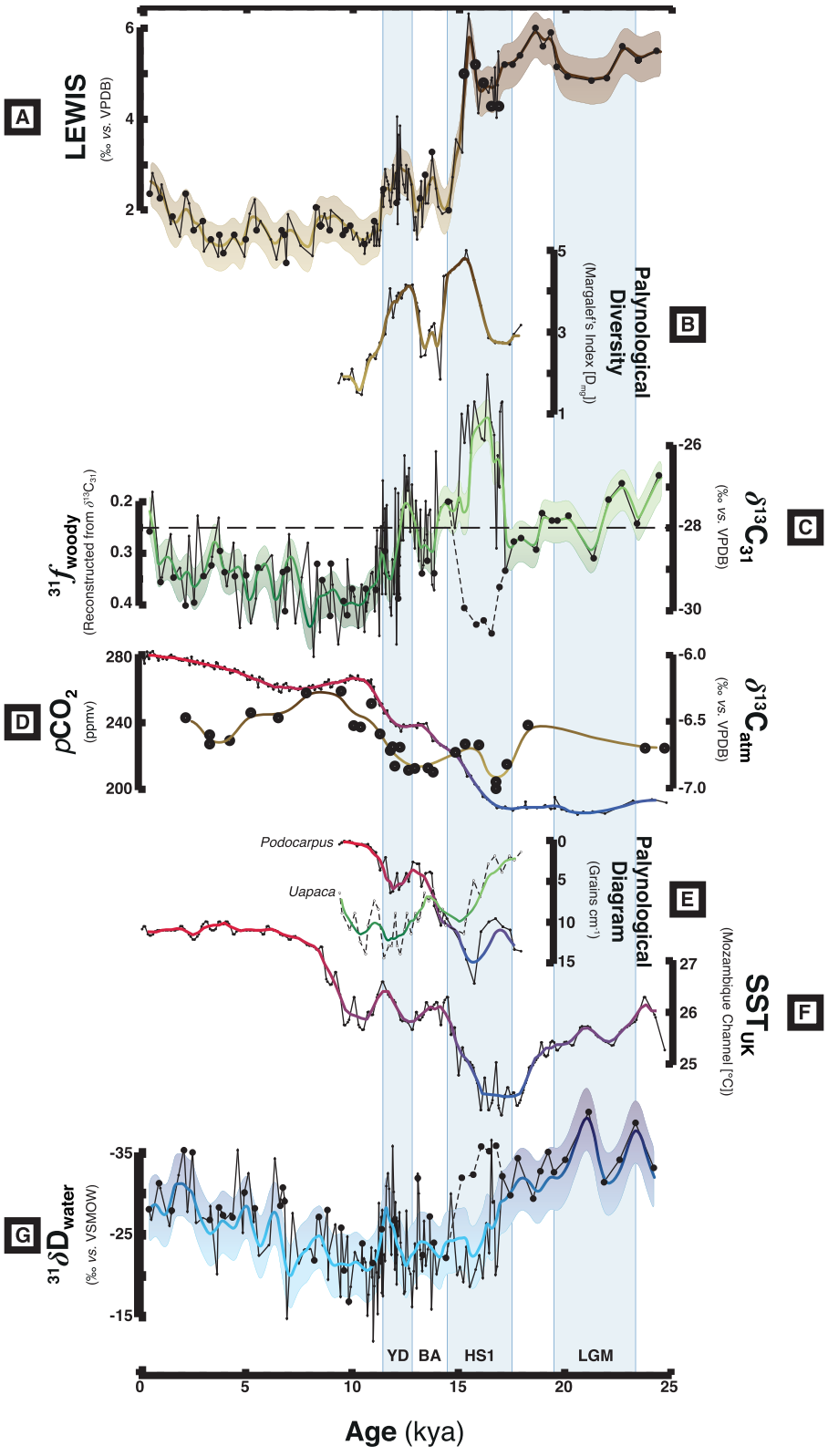


**Fig 5. Downcore records of environmental change in southeast Africa over the last 25 kya. A**, Sediment LEWIS (Discussion G in S1 File) for correlative marine cores recovered from off the Zambezi River mouth [GeoB9307 (filled circles) [39]; GIK16160 (open circles) [40]], which reflect the changing plant species richness of lower Zambezi

vegetation communities [39]. Shaded bold lines show a combined 250-yr Gaussian smoothed time-series. Shaded bounds indicate empirical 90% confidence intervals as calculated from a Monte Carlo method [92]. **B**, Pollen-inferred biodiversity patterns at Lake Malawi [57] as shown with Margalef's Index ($D_{mg} = [G- 1][\ln N]^{-1}$ where $G$ is the cumulative number of taxa [e.g., genera] in a sample and $N$ is the corresponding pollen sum) [63], which has a strong positive correlation with species richness at landscape scales [58, 62]. **C**, Downcore records of $\delta^{13}C_{31}$ values, which are indicative of $C_3/C_4$ plant functional type dominance [35]. Associated $\delta^{13}C_{31}$ values were also used to reconstruct fractional tree cover [$^{31}f_{woody}$ (dashed lines)] through time (Discussion D in S1 File). **D**, Atmospheric carbon dioxide concentrations ($pCO_2$) and its stable carbon isotopic composition ($\delta^{13}C_{atm}$) as recorded by polar ice [93], and the **E**, Pollen abundance diagram of *Podocarpus*, which is an indirect temperature indicator, and *Uapaca* and at Lake Malawi [57]. **F**, Downcore alkenone-estimates of the sea surface temperature ($SST_{UK}$) for at GIK16160 [94], which is representative of temperature changes in the lower Zambezi sub-catchment [39]. **G**, Downcore records of the stable hydrogen isotopic composition in water used by plants [$^{31}\delta D_{water}$ (Discussion E in S1 File)] reconstructed from $n$-$C_{31}\delta D$ values in sediments at GeoB9307 (filled circles) [39] and GIK16160 (open circles) [40], representing precipitation changes in the lower Zambezi sub-catchment [39]. Lower $^{31}\delta D_{water}$ values are indicative of higher rainfall related to changes in monsoon intensity [48]. Abbreviations are written as: Younger Dryas (YD); Heinrich Stadial 1 (H1); Bolling-Allerød (BA); Last Glacial Maximum (LGM).

https://doi.org/10.1371/journal.pone.0212211.g005

kya [56–59]. In part, this seeming paradox may reflect the varied taxonomic resolution inherent to many pollen spectra [30]; though higher rank biodiversity parallels species richness under certain conditions, contemporary pollen spectra reflect (paleo)vegetation dynamics across a range of disparate area and time scales [60]. Consequently, pollen records can obscure important biodiversity patterns [53] and functional trait divergence at lower rank [61] that biomarker signatures can reveal by proxy [11, 55, 62]. This said, in our study, plant biodiversity is defined by published literature estimates of the observed taxonomic richness in specific (sub)tropical African ecoregions, which might demarcate expressly quantitative interpretations of LEWIS because ancient African savannahs might have differed in composition or structure as compared to modern analogues [5, 59]. Even still, the strong positive relationship species richness shows with sediment LEWIS forges a conceptual link between existing pollen and biomarker records, which allows us to differentiate changes in community production (e.g., plant biomass), ecosystem structure and biodiversity.

During glacial termination, about ~25–17.5 kya, reconstructed fractional tree cover ($^{31}f_{woody}$) estimates of 0.25±0.10 (Fig 5C) occur in conjunction with high pollen abundances among grasses and highland taxa (e.g., *Podocarpus* [Fig 5E]) [56]. High sediment LEWIS values also occur throughout this interval (Fig 5A) that, together with high corresponding palynological diversity ($D_{mg}$) [63], denote species-rich vegetation communities with irregular crown cover and highly productive understory grasses, characteristic of African miombo woodlands [64].

High sediment LEWIS values and $D_{mg}$ continued from ~17.5–15 kya (Fig 5A and 5B, respectively), but fractional tree cover estimates skewed to more extreme values (Fig 5C and Discussion H in S1 File). Amid Heinrich Stadial 1 [HS1 (17.5–14.7 kya)], the increasing pollen abundances of deciduous woodland taxa (e.g., *Uapaca* [Fig 5E]) [57, 58] indicate a shift toward Zambezian woodland-like vegetation communities [64], which are characterized by patches of dry-deciduous woody plants surrounded by grasses. Then, a dramatic decrease in sediment LEWIS values and $D_{mg}$ occurs at the HS1–Bolling-Allerød (BA; 14.7–12.9 kya) transition alongside smaller increases in reconstructed fractional tree cover and the abundance of tropical forest taxa (e.g., *Macaranga*-type pollen) [58] together suggest the sudden expansion of less species-rich vegetation communities, such as mopane woodlands [22, 64].

Sediment LEWIS values and $D_{mg}$ increase again around 12.9–11.7 kya [i.e., Younger Dryas (YD)], but low sediment LEWIS values during the earliest Holocene mirror reconstructed fractional tree cover and deciduous woodland taxa abundances [56, 57] that together are suggestive of the *Acacia-Combretum* woodlands [64] common in the lower Zambezi today [65]. The end-Holocene reconstructed fractional tree cover of 0.43 (S1 Table) is consistent with

recent MODIS tree cover estimates of ~0.40 for the lower Zambezi sub-catchment (Discussion H in S1 File) [66, 67], and further supports our use of $\delta^{13}C_{31}$ values as a reflection of PFT dominance and fractional tree cover.

The maximum isotopic difference demonstrated between end-member abundance-weighted $\delta^{13}C_{29}$ and $\delta^{13}C_{33}$ values of ~4.8‰ defines an internal benchmark of higher conceptual LEWIS index values apart from additional bioclimatic influences. Indeed, (micro)habitat heterogeneities in ecoregion structure could lead to additional differences of 3–4‰ between savannahs with homogenous PFT distributions as compared to relatively patchier ones [35]. This conceptual difference is corroborated by previous studies noting plant biodiversity parallels increasing patchiness even in savannahs with identical fractional tree cover estimates at the landscape scale (Discussion G in S1 File).

Beyond internal (micro)habitat influences on the carbon isotopic composition of leaf-waxes, major climatic controls on savannah vegetation communities are related to changes in rainfall, temperature, and $pCO_2$ [68] though their relative importance can differ with observation scale [69]. For instance, equilibrium vegetation model (BIOME4) simulations [68] suggest that lower Zambezi ecosystem structure was controlled by $pCO_2$ during glacial termination until ~10 kya (Fig 5D), but that temperature and, to a much lesser degree, rainfall together controlled Holocene succession (Fig 5F and 5G). These respective simulations are corroborative with the moderate correlation strength apparent between reconstructed fractional tree cover estimates ($^{31}f_{woody}$) and: (*i*) $pCO_2$ during glacial termination and ~10 kya ($r = 0.647$), and (*ii*) reconstructed late-summer (austral) temperatures since ~10 kya ($r = -0.714$). Collectively, $pCO_2$ and temperature explains 61% of the downcore variance in reconstructed fractional tree cover in a multiple regression model (Discussion I in S1 File).

Sediment LEWIS values share a relationship with corresponding $pCO_2$ ($r = -0.940$) that does not become stronger in multiple regression models with a secondary predictor (Discussion I in S1 File). This correlation cannot be a simple consequence of increasing $pCO_2$ on apparent $C_3$ plant fractionation (Discussion G in S1 File) through the deglacial transition since such increases should have a negligible influence on carbon isotope discrimination in coincident $C_4$ plants [70]. Rather, we suggest increasing $pCO_2$ prompted decreasing plant functional trait divergence [71, 72] and, in turn, decreased biodiversity at the regional level [73]. For instance, increasing $pCO_2$ promotes increased $C_3$ photosynthetic water use efficiency [74], particularly plants with woody growth forms and forbs [75, 76], and thereby promotes decreased levels of facilitative-competitive interactions vis-à-vis resource-use strategies (i.e., water, carbon and light) [28, 77]. Resource-use strategies underlay plant functional trait divergence [77], which in turn underlies most differences in carbon isotope discrimination among populations (intraspecific) and between species [78, 79]. All things considered, this mechanism suggests increasing $pCO_2$ prompts decreased LEWIS values as a consequence of decreased functional trait divergence (i.e., decreased PSR) and its effects on carbon isotope discrimination [79], which are related to resource use [41, 78]. Such a mechanism is consistent with the results of leaf-level function models [28], experimental data [80], and the consequences of increasing $pCO_2$ on savannah biodiversity under modelled business-as-usual future climate scenarios within the next 100 years [81].

Even though these results indicate sediment LEWIS tracks changing plant biodiversity, there are some important limitations in our approach. For instance, isotopic responses of differing plant types are consequent to *interactive* effects of bioclimatic variables [68, 82], and furthermore are often species specific [83]. Indeed, plants show complex variation in their ecophysiological, biosynthetic, and molecular responsiveness to changing $pCO_2$ over a wide range of timescales [76, 83]. These complexities underscore a caveat to our interpretations, as does recent literature about $C_3$ plants re-assimilating photorespired $CO_2$ [84], since each could

have unpredictable effects on apparent landscape-scale carbon isotope discrimination. Our multivariate analyses also do not take into account the unpredictable effects of changing $pCO_2$ on evolutionary processes [83] or environmental (historical) hysteresis [28], which can influence stable carbon isotopic composition of leaf biomass [82]. Even so, numerous studies suggest Quaternary plant biodiversity patterns were dominantly guided by (paleo)environmental influences on ecohydrological (functional) trait divergence [80, 85], suggesting post-LGM PSR trends are explicitly predictable using paired bioclimatic constraints and LEWIS.

In recent decades, intense debate has arisen about tropical biodiversity patterns during periods of far-reaching global warming, such as during glacial terminations and future climate scenarios [83]. This research develops a novel tool for reconstructions and, theoretically, projections of the species richness in savannah ecosystems at disparate area and time (i.e., integration) scales. Conservatively, $pCO_2$ is modelled to reach 550–800 p.p.m.v. around 2050 and 2080, respectively [86]. The relative magnitude of this increase in concentration is comparable with the increasing $pCO_2$ between about 17 kya and 10 kya (Fig 5D) that featured dramatic declines in species richness of Zambezi vegetation communities (Fig 5A and 5B). If the scaling (power) relationship present between species richness as compared to surface-sediment LEWIS (Fig 4) holds during past and future climate change events, anticipated impending $pCO_2$ jumps will drive an estimated local loss of 1000±750 Zambezian species of flowering plants, which is at the extreme of terrestrial biodiversity privation estimates, on average, worldwide [87, 88]. Considering plant biodiversity exerts a direct influence on organic carbon storage [2] and terrestrial discharge [58] from drylands such as savannas [89], our results establish further motivation for in-depth investigation of the effects of future anthropogenic emission scenarios [81, 90]–particularly in relation to woody plant encroachment [91].

## Supporting information

**S1 File.** This appendix contains supporting discussions (Discussions A–J) together with supporting figures (Figures A–F).
(PDF)

**S1 Table. Median and median absolute deviation values of $C_{27}$–$C_{33}$ *n*-alkane $\delta^{13}C$ data and LEWIS values in contemporary plant leaves.**
(XLS)

**S2 Table. Surface-sediment locations alongside characteristics of their respective source (eco)regions, surface material terms, species–time–area relationship variables, measured $C_{27}$–$C_{33}$ *n*-alkane $\delta^{13}C$ values, LEWIS values, and fractional tree cover estimates.**
(XLS)

**S3 Table. Measured biomarker *n*-alkane $\delta^{13}C$ values and LEWIS values in sediment cores recovered from off the Zambezi River mouth.**
(XLS)

## Author Contributions

**Conceptualization:** Clayton R. Magill, Geoffrey Eglinton, Timothy I. Eglinton.

**Formal analysis:** Geoffrey Eglinton.

**Investigation:** Clayton R. Magill.

**Methodology:** Clayton R. Magill, Geoffrey Eglinton.

**Resources:** Timothy I. Eglinton.

**Visualization:** Clayton R. Magill, Geoffrey Eglinton.

**Writing – original draft:** Clayton R. Magill, Geoffrey Eglinton, Timothy I. Eglinton.

**Writing – review & editing:** Clayton R. Magill, Geoffrey Eglinton, Timothy I. Eglinton.

## References


1. Hooper DU, Solan M, Symstad A, Diaz S, Gessner MO, Buchmann N, et al. Species diversity, functional diversity and ecosystem functioning. In: Inchausti P, Loreau M, Naeem S, editors. Biodiversity and Ecosystem Functioning: Synthesis and Perspectives Oxford: Oxford University Press Oxford, UK; 2002. p. 195–208.
2. Maestre FT, Quero JL, Gotelli NJ, Escudero A, Ochoa V, Delgado-Baquerizo M, et al. Plant species richness and ecosystem multifunctionality in global drylands. Science. 2012; 335(6065):214–8. https://doi.org/10.1126/science.1215442 PMID: 22246775
3. Valentini R, Arneth A, Bombelli A, Castaldi S, Cazzolla Gatti R, Chevallier F, et al. A full greenhouse gases budget of Africa: synthesis, uncertainties, and vulnerabilities. Biogeosciences. 2014; 11(2):381–407. https://doi.org/10.5194/bg-11-381-2014
4. Calvo MM, Prentice IC. Effects of fire and $CO_2$ on biogeography and primary production in glacial and modern climates. New Phytol. 2015; 208(3):987–94. https://doi.org/10.1111/nph.13485 PMID: 26033154
5. Maguire KC, Nieto-Lugilde D, Fitzpatrick MC, Williams JW, Blois JL. Modeling species and community responses to past, present, and future episodes of climatic and ecological change. Annu Rev Ecol Evol S. 2015; 46:343–68.
6. Broennimann O, Thuiller W, Hughes G, Midgley GF, Alkemade JMR, Guisan A. Do geographic distribution, niche property and life form explain plants' vulnerability to global change? Glob Change Biol. 2006; 12(6):1079–93.
7. Loreau M, Naeem S, Grime P. Inchausti J. P., Raffaelli Hooper D, Inchausti P, Bengtsson J. Biodiversity and Ecosystem Functioning: Current Knowledge and Future Challenges. Science. 2001; 294 (5543):804–8. https://doi.org/10.1126/science.1064088 PMID: 11679658
8. Birks HJB, Felde VA, Bjune AE, Grytnes J-A, Seppä H, Giesecke T. Does pollen-assemblage richness reflect floristic richness? A review of recent developments and future challenges. Rev Palaeobot Palyno. 2016; 228:1–25.
9. Goring S, Lacourse T, Pellatt MG, Mathewes RW. Pollen assemblage richness does not reflect regional plant species richness: a cautionary tale. J Ecol. 2013; 101(5):1137–45.
10. Campbell ID. Quaternary pollen taphonomy: examples of differential redeposition and differential preservation. Palaeogeogr Palaeocl. 1999; 149(1):245–56.
11. Castañeda IS, Caley T, Dupont L, Kim J-H, Malaizé B, Schouten S. Middle to Late Pleistocene vegetation and climate change in subtropical southern East Africa. Earth Planet Sc Lett. 2016; 450:306–16.
12. Koellner T, de Baan L, Beck T, Brandão M, Civit B, Margni M, et al. UNEP-SETAC guideline on global land use impact assessment on biodiversity and ecosystem services in LCA. The International Journal of Life Cycle Assessment. 2013; 18(6):1188–202. https://doi.org/10.1007/s11367-013-0579-z
13. Hoffmann WA, Geiger EL, Gotsch SG, Rossatto DR, Silva LCR, Lau OL, et al. Ecological thresholds at the savanna-forest boundary: how plant traits, resources and fire govern the distribution of tropical biomes. Ecol Lett. 2012; 15(7):759–68. https://doi.org/10.1111/j.1461-0248.2012.01789.x PMID: 22554474
14. Cowling RM, Esler KJ, Midgley GF, Honig MA. Plant functional diversity, species diversity and climate in arid and semi-arid southern Africa. J Arid Environ. 1994; 27(2):141–58. https://doi.org/10.1006/jare.1994.1054
15. Skarpe C. Plant functional types and climate in a southern African savanna. J Veg Sci. 1996; 7(3):397–404.
16. House JI, Archer S, Breshears DD, Scholes RJ. Conundrums in mixed woody–herbaceous plant systems. J Biogeogr. 2003; 30(11):1763–77.
17. Belsky AJ, Amundson RG, Duxbury JM. The effects of trees on their physical, chemical and biological environments in a semi-arid savanna in Kenya. J Appl Ecol. 1989; 26:1005–24.
18. Peterson DW, Reich PB. Fire frequency and tree canopy structure influence plant species diversity in a forest-grassland ecotone. Plant Ecol. 2007; 194(1):5–16. https://doi.org/10.1007/s11258-007-9270-4

19. Soliveres S, Maestre FT, Eldridge DJ, Delgado-Baquerizo M, Quero JL, Bowker MA, et al. Plant diversity and ecosystem multifunctionality peak at intermediate levels of woody cover in global drylands. Global Ecol Biogeogr. 2014; 23(12):1408–16. https://doi.org/10.1111/geb.12215 PMID: 25914607

20. Shirima DD, Totland Ø, Munishi PKT, Moe SR. Relationships between tree species richness, evenness and aboveground carbon storage in montane forests and miombo woodlands of Tanzania. Basic Appl Ecol. 2015; 16(3):239–49.

21. Whittaker RJ, Willis KJ, Field R. Scale and species richness: towards a general theory of species diversity hierarchical. J Biogeogr. 2001; 28(4):453–70. https://doi.org/10.1046/j.1365-2699.2001.00563.x

22. Kier G, Mutke J, Dinerstein E, Ricketts TH, Küper W, Kreft H, et al. Global patterns of plant diversity and floristic knowledge. J Biogeogr. 2005; 32(7):1107–16. https://doi.org/10.1111/j.1365-2699.2005.01272.x

23. Scheiner SM, Chiarucci A, Fox GA, Helmus MR, McGlinn DJ, Willig MR. The underpinnings of the relationship of species richness with space and time. Ecol Monogr. 2011; 81(2):195–213.

24. Araya YN, Silvertown J, Gowing DJ, McConway KJ, Peter Linder H, Midgley G. A fundamental, eco-hydrological basis for niche segregation in plant communities. New Phytol. 2011; 189(1):253–8. https://doi.org/10.1111/j.1469-8137.2010.03475.x PMID: 20868394

25. Sala OE, Lauenroth WK, Golluscio RA. Plant functional types in temperate semi-arid regions. In: Smith TM, Shugart HH, Woodward FI, editors. Plant functional types: their relevance to ecosystem properties and global change: Cambridge University Press; 1997. p. 217–33.

26. Roscher C, Schumacher J, Lipowsky A, Gubsch M, Weigelt A, Pompe S, et al. A functional trait-based approach to understand community assembly and diversity–productivity relationships over 7 years in experimental grasslands. Perspect Plant Ecol. 2013; 15(3):139–49.

27. Mitchell N, Moore TE, Mollmann HK, Carlson JE, Mocko K, Martinez-Cabrera H, et al. Functional traits in parallel evolutionary radiations and trait-environment associations in the cape floristic region of South Africa. Am Nat. 2015; 185(4):525–37. https://doi.org/10.1086/680051 PMID: 25811086

28. Higgins SI, Scheiter S. Atmospheric $CO_2$ forces abrupt vegetation shifts locally, but not globally. Nature. 2012; 488(7410):209–12. https://doi.org/10.1038/nature11238 PMID: 22763447

29. Colgan MS, Martin RE, Baldeck CA, Asner GP. Tree foliar chemistry in an African savanna and its relation to life history strategies and environmental filters. PLoS One. 2015; 10(5):e0124078–e. https://doi.org/10.1371/journal.pone.0124078 PMID: 25993539

30. Odgaard BV. Fossil pollen as a record of past biodiversity. J Biogeogr. 1999; 26(1):7–17.

31. Eglinton TI, Eglinton G. Molecular proxies for paleoclimatology. Earth Planet Sc Lett. 2008; 275:1–16.

32. Rommerskirchen F, Plader A, Eglinton G, Chikaraishi Y, Rullkötter J. Chemotaxonomic significance of distribution and stable carbon isotopic composition of long-chain alkanes and alkan-1-ols in C4 grass waxes. Org Geochem. 2006; 37(10):1303–32. https://doi.org/10.1016/j.orggeochem.2005.12.013

33. Vogts A, Moossen H, Rommerskirchen F, Rullkötter J. Distribution patterns and stable carbon isotopic composition of alkanes and alkan-1-ols from plant waxes of African rain forest and savanna C3 species. Org Geochem. 2009; 40(10):1037–54.

34. Bush RT, McInerney FA. Leaf wax n-alkane distributions in and across modern plants: implications for paleoecology and chemotaxonomy. Geochim Cosmochim Ac. 2013; 117:161–79.

35. Magill CR, Ashley GM, Freeman KH. Ecosystem variability and early human habitats in eastern Africa. P Natl Acad Sci USA. 2013; 110(4):1167–74.

36. Magill CR, Ashley GM, Domínguez-Rodrigo M, Freeman KH. Dietary options and behavior suggested by plant biomarker evidence in an early human habitat. P Natl Acad Sci USA. 2016; 113(11):2874–9.

37. Hemingway JD, Schefuß E, Dinga BJ, Pryer H, Galy VV. Multiple plant-wax compounds record differential sources and ecosystem structure in large river catchments. Geochim Cosmochim Ac. 2016; 184:20–40.

38. Bush RT, Wallace J, Currano ED, Jacobs BF, McInerney FA, Dunn RE, et al. Cell anatomy and leaf $\delta^{13}C$ as proxies for shading and canopy structure in a Miocene forest from Ethiopia. Palaeogeogr Palaeocl. 2017; 485(Supplement C):593–604. https://doi.org/10.1016/j.palaeo.2017.07.015.

39. Schefuß E, Kuhlmann H, Mollenhauer G, Prange M, Pätzold J. Forcing of wet phases in southeast Africa over the past 17,000 years. Nature. 2011; 480(7378):509–12. https://doi.org/10.1038/nature10685 PMID: 22193106

40. Wang YV, Larsen T, Leduc G, Andersen N, Blanz T, Schneider RR. What does leaf wax δD from a mixed C3/C4 vegetation region tell us? Geochim Cosmochim Ac. 2013; 111:128–39. https://doi.org/10.1016/j.gca.2012.10.016

41. Westoby M, Falster DS, Moles AT, Vesk PA, Wright IJ. Plant ecological strategies: some leading dimensions of variation between species. Annu Rev Ecol Syst. 2002:125–59.

42. Magill CR, Denis EH, Freeman KH. Rapid sequential separation of sedimentary lipid biomarkers via selective accelerated solvent extraction. Org Geochem. 2015; 88:29–34.

43. Sadler PM, Jerolmack DJ. Scaling laws for aggradation, denudation and progradation rates: the case for time-scale invariance at sediment sources and sinks. Geol Soc Spec Publ. 2014; 404(1):SP404.7–SP.7. https://doi.org/10.1144/SP404.7

44. Brooks JR, Flanagan LB, Buchmann N, Ehleringer JR. Carbon isotope composition of boreal plants: functional grouping of life forms. Oecologia. 1997; 110(3):301–11. https://doi.org/10.1007/s004420050163 PMID: 28307218

45. Chen S, Bai Y, Lin G, Han X. Variations in life-form composition and foliar carbon isotope discrimination among eight plant communities under different soil moisture conditions in the Xilin River Basin, Inner Mongolia, China. Ecol Res. 2005; 20(2):167–76.

46. Lloyd J, Bird MI, Vellen L, Miranda AC, Veenendaal EM, Djagbletey G, et al. Contributions of woody and herbaceous vegetation to tropical savanna ecosystem productivity: a quasi-global estimate. Tree Physiol. 2008; 28(3):451–68. PMID: 18171668

47. Krull ES, Skjemstad JO, Burrows WH, Bray SG, Wynn JG, Bol R, et al. Recent vegetation changes in central Queensland, Australia: evidence from $\delta^{13}C$ and 14C analyses of soil organic matter. Geoderma. 2005; 126(3):241–59. https://doi.org/10.1016/j.geoderma.2004.09.012

48. Magill CR, Ashley GM, Freeman KH. Water, plants, and early human habitats in eastern Africa. P Natl Acad Sci USA. 2013; 110(4):1175–80.

49. Kelly CK, Woodward FI. Ecological correlates of carbon isotope composition of leaves: a comparative analysis testing for the effects of temperature, CO2 and O2 partial pressures and taxonomic relatedness on $\delta^{13}C$. J Ecol. 1995; 83(3):509–15. https://doi.org/10.2307/2261603

50. Breshears DD. The grassland-forest continuum: Trends in ecosystem properties for woody plant mosaics? Front Ecol Environ. 2006; 4(Fig 2):96–104. https://doi.org/10.1890/1540-9295(2006)004[0096:TGCTIE]2.0.CO;2

51. Hüttich C, Herold M, Strohbach BJBJ, Dech S. Integrating in-situ, Landsat, and MODIS data for mapping in Southern African savannas: experiences of LCCS-based land-cover mapping in the Kalahari in Namibia. Environ Monit Assess. 2011; 176(1–4):531–47. https://doi.org/10.1007/s10661-010-1602-5 PMID: 20635199

52. De Vente J, Poesen J. Predicting soil erosion and sediment yield at the basin scale: scale issues and semi-quantitative models. Earth-Sci Rev. 2005; 71(1):95–125.

53. Letters E, Gotelli NJ, Colwell RK, Letters E. Quantifying biodiversity: procedures and pitfalls in the measurement and comparison of species richness. Ecol Lett. 2001; 4(May 1988):379–91.

54. Moya-Laraño J, Corcobado G. Plotting partial correlation and regression in ecological studies. Web Ecol. 2008; 8(1):35–46. https://doi.org/10.5194/we-8-35-2008

55. Castañeda IS, Werne JP, Johnson TC, Filley TR. Late Quaternary vegetation history of southeast Africa: the molecular isotopic record from Lake Malawi. Palaeogeogr Palaeocl. 2009; 275(1):100–12.

56. DeBusk GH. A 37,500-year pollen record from Lake Malawi and implications for the biogeography of afromontane forests. J Biogeogr. 1998; 25:479–500.

57. Ivory SJ, Lézine A- M, Vincens A, Cohen AS. Effect of aridity and rainfall seasonality on vegetation in the southern tropics of East Africa during the Pleistocene/Holocene transition. Quaternary Res. 2012; 77(1):77–86.

58. Ivory SJ, McGlue MM, Ellis GS, Lézine A- M, Cohen AS, Vincens A. Vegetation controls on weathering intensity during the last deglacial transition in southeast Africa. PLoS One. 2014; 9(11):e112855–e. https://doi.org/10.1371/journal.pone.0112855 PMID: 25406090

59. Daru BH, Bank M, Maurin O, Yessoufou K, Schaefer H, Slingsby JA, et al. A novel phylogenetic regionalization of phytogeographical zones of southern Africa reveals their hidden evolutionary affinities. J Biogeogr. 2016; 43(1):155–66.

60. Sugita S. Pollen representation of vegetation in Quaternary sediments: theory and method in patchy vegetation. J Ecol. 1994; 82(4):881–97.

61. Mander L, Punyasena SW. On the taxonomic resolution of pollen and spore records of Earth's vegetation. Int J Plant Sci. 2014; 175(8):931–45.

62. Ivory SJ, Russell J. Climate, herbivory, and fire controls on tropical African forest for the last 60ka. Quaternary Science Reviews. 2016; 148(Supplement C):101–14. https://doi.org/10.1016/j.quascirev.2016.07.015.

63. Margalef R, Gutierrez E. How to introduce connectance in the frame of an expression for diversity. Am Nat. 1983:601–7.

64. Timberlake J. Biodiversity of the Zambezi Basin. Occas Publ Biodivers. 2000; 9(9):1–22.

65. Burrough SL, Willis KJ. Ecosystem resilience to late-Holocene climate change in the Upper Zambezi Valley. Holocene. 2015; 25(11):1811–28. https://doi.org/10.1177/0959683615591355

66. Sexton JO, Song X-P, Feng M, Noojipady P, Anand A, Huang C, et al. Global, 30-m resolution continuous fields of tree cover: Landsat-based rescaling of MODIS vegetation continuous fields with lidar-based estimates of error. Int J Digit Earth. 2013; 6(5):427–48. https://doi.org/10.1080/17538947.2013.786146

67. Ryan CM, Williams MM, Hill TC, Grace J, Woodhouse IH. Assessing the phenology of southern tropical Africa: a comparison of hemispherical photography, scatterometry, and optical/NIR remote sensing. IEEE T Geosci Remote. 2014; 52(1):519–28. https://doi.org/10.1109/TGRS.2013.2242081

68. Khon VC, Wang YV, Krebs-Kanzow U, Kaplan JO, Schneider RR, Schneider B. Climate and CO2 effects on the vegetation of southern tropical Africa over the last 37,000 years. Earth Planet Sc Lett. 2014; 403(0):407–17. http://dx.doi.org/10.1016/j.epsl.2014.06.043.

69. O'Connor TG, Haines LM, Snyman HA. Influence of precipitation and species composition on phytomass of a semi-arid African grassland. J Ecol. 2001; 89(5):850–60. https://doi.org/10.1046/j.0022-0477.2001.00605.x

70. Schubert BA, Jahren AH. Global increase in plant carbon isotope fractionation following the Last Glacial Maximum caused by increase in atmospheric pCO2. Geology. 2015; 43(5):435–8.

71. Nicotra ABAB Atkin OKOK, Bonser SPSP, Davidson AM, Finnegan EJ, Mathesius U, et al. Plant phenotypic plasticity in a changing climate. Trends Plant Sci. 2010; 15(12):684–92. https://doi.org/10.1016/j.tplants.2010.09.008 PMID: 20970368

72. Dalerum F, Cameron EZ, Kunkel K, Somers MJ. Interactive effects of species richness and species traits on functional diversity and redundancy. Theor Ecol. 2012; 5(1):129–39.

73. Anderson TM, Metzger KL, McNaughton SJ, Michael Anderson T, Metzger KL, McNaughton SJ. Multiscale analysis of plant species richness in Serengeti grasslands. J Biogeogr. 2007; 34(2):313–23. https://doi.org/10.1111/j.1365-2699.2006.01598.x

74. Franco AC, Rossatto DR, Silva LdCR, da Silva Ferreira C. Cerrado vegetation and global change: the role of functional types, resource availability and disturbance in regulating plant community responses to rising CO2 levels and climate warming. Theor Exp Plant Physiol. 2014; 26(1):19–38.

75. Ainsworth EA, Long SP. What have we learned from 15 years of free-air CO2 enrichment (FACE)? A meta-analytic review of the responses of photosynthesis, canopy properties and plant production to rising $CO_2$. New Phytol. 2005; 165(2):351–72. https://doi.org/10.1111/j.1469-8137.2004.01224.x PMID: 15720649

76. Polley HW, Jin VL, Fay PA. $CO_2$-caused change in plant species composition rivals the shift in vegetation between mid-grass and tallgrass prairies. Glob Change Biol. 2012; 18(2):700–10.

77. Callaway RM, Pennings SC, Richards CL. Phenotypic plasticity and interactions among plants. Ecology. 2003; 84(5):1115–28.

78. Tsialtas JT, Handley LL, Kassioumi MT, Veresoglou DS, Gagianas AA. Interspecific variation in potential water-use efficiency and its relation to plant species abundance in a water-limited grassland. Funct Ecol. 2001; 15(5):605–14.

79. Kahmen A, Perner J, Buchmann N. Diversity-dependent productivity in semi-natural grasslands following climate perturbations. Funct Ecol. 2005; 19(4):594–601.

80. Silvertown J, Araya Y, Gowing D. Hydrological niches in terrestrial plant communities: a review. J Ecol. 2015; 103(1):93–108. https://doi.org/10.1111/1365-2745.12332

81. Sala OE, Chapin FS, Armesto JJ, Berlow E, Bloomfield J, Dirzo R, et al. Global biodiversity scenarios for the year 2100. Science. 2000; 287(5459):1770–4. PMID: 10710299

82. Cernusak LA, Ubierna N, Winter K, Holtum JAM, Marshall JD, Farquhar GD. Environmental and physiological determinants of carbon isotope discrimination in terrestrial plants. New Phytol. 2013; 200(4):950–65. https://doi.org/10.1111/nph.12423 PMID: 23902460

83. Leakey ADB, Lau JA. Evolutionary context for understanding and manipulating plant responses to past, present and future atmospheric [CO2]. Philos T Roy Soc B. 2012; 367(1588):613–29.

84. Busch FA, Sage TL, Cousins AB, Sage RF. C3 plants enhance rates of photosynthesis by reassimilating photorespired and respired CO2. Plant Cell Environ. 2013; 36(1):200–12. https://doi.org/10.1111/j.1365-3040.2012.02567.x PMID: 22734462

85. Kleidon A, Adams J, Pavlick R, Reu B. Simulated geographic variations of plant species richness, evenness and abundance using climatic constraints on plant functional diversity. Environ Res Lett. 2009; 4(1):14007–.

86. Deryng D, Elliott J, Folberth C, Müller C, Pugh TAM, Boote KJ, et al. Regional disparities in the beneficial effects of rising CO2 concentrations on crop water productivity. Nature Clim Change. 2016; 6:786–90.

87. Solomon S, Qin D, Manning M, Chen Z, Marquis M, Averyt KB, et al. Contribution of working group I to the fourth assessment report of the intergovernmental panel on climate change, 2007. Cambridge University Press, Cambridge; 2007.

88. Heubes J, Schmidt M, Stuch B, Márquez JRG, Wittig R, Zizka G, et al. The projected impact of climate and land use change on plant diversity: an example from West Africa. J Arid Environ. 2013; 96:48–54.

89. Grace J, Jose JS, Meir P, Miranda HS, Montes RA. Productivity and carbon fluxes of tropical savannas. J Biogeogr. 2006; 33(3):387–400. https://doi.org/10.1111/j.1365-2699.2005.01448.x

90. Gill RA, Polley HW, Johnson HB, Anderson LJ, Maherali H, Jackson RB. Nonlinear grassland responses to past and future atmospheric CO2. Nature. 2002; 417(6886):279–82. https://doi.org/10.1038/417279a PMID: 12015601

91. Jackson RB, Banner JL, Jobbágy EG, Pockman WT, Wall DH. Ecosystem carbon loss with woody plant invasion of grasslands. Nature. 2002; 418(6898):623–6. https://doi.org/10.1038/nature00910 PMID: 12167857

92. Anchukaitis KJ, Tierney JE. Identifying coherent spatiotemporal modes in time-uncertain proxy paleoclimate records. Clim Dynam. 2013; 41(5–6):1291–306.

93. Monnin E, Indermühle A, Dällenbach A, Flückiger J, Stauffer B, Stocker TF, et al. Atmospheric CO2 concentrations over the last glacial termination. Science. 2001; 291(5501):112–4. https://doi.org/10.1126/science.291.5501.112 PMID: 11141559

94. Wang YV, Leduc G, Regenberg M, Andersen N, Larsen T, Blanz T, et al. Northern and southern hemisphere controls on seasonal sea surface temperatures in the Indian Ocean during the last deglaciation. Paleoceanography. 2013; 28(4):619–32. https://doi.org/10.1002/palo.20053